BER versus Data Rate Performance of SCM Transmission over Multimode Fibers at Low-Frequency Passbands with Linear Block Codes

Jaruwat Patmanee[1] and Surachet Kanprachar[2*]
[1] Faculty of Logistics and Digital Supply Chain, Naresuan University, Phitsanulok, Thailand
[2] Faculty of Engineering, Naresuan University, Phitsanulok, Thailand
Email: surachetka@nu.ac.th

Abstract—The use of Multimode fibers (MMFs) in the low-frequency region has been studied. It is found that many available low-frequency passbands can be used as channels. However, these passbands are frequency-selective channels, which can negatively affect to the transmitted signal. To lessen this effect, Linear Block Code (LBC) along with a careful selection of passbands is applied. In this work, the performance in terms of BER and data rate for an MMF communication system using a 1-km length MMF at low-frequency passbands with different schemes of LBC is studied. This study uses subcarrier multiplexing (SCM) with a 3-dB modal bandwidth and other low-frequency passbands as channels. The results show that by using (31, 26) LBC and Type-I bit allocation, a data rate of 494 Mbps can be obtained with a BER lower than 10^{-9}. Moreover, a BER lower than 10^{-14} can be achieved with a data rate of 399 Mbps, which is two-fold higher than the data rate obtained using only the 3-dB modal bandwidth. Additionally, the BER versus data rate for different cases in terms of applying LBC to the system are found and can be practically used as a guideline in selecting a BER and data rate that are suitable for the minimum requirement of a given communication system.

Index Terms—Bit error rate, data rate, linear block code, multimode fibers, passbands, subcarrier multiplexing

I. Introduction

Multimode fiber (MMF) is one type of optical fiber. There are many guided modes in this kind of fiber [1]. Optical communication systems using multimode fibers are the most popular communication systems worldwide. They are widely used for short-haul communication, such as indoor communication and communication between buildings. However, the 3-dB modal bandwidth, which is the most commonly used multimode fiber, is limited to 200-500 MHz·km, depending on the fiber type, length, and other characteristics. To overcome this limitation, selective mode excitation [2]-[4], which is one kind of Mode Division Multiplexing (MDM), has been studied. Selective mode excitation aims to excite only a specific mode or the polarization of a mode. Thus, the frequency response of MMF is more stable because of the limited number of modes, resulting in a wider 3-dB modal bandwidth. Additionally, during signal transmission using MDM, the complex distortion of the light field can be exploited. It is resulting in difficult challenges to decode the transmitted data, yielding an enhancement of information security [5], [6]. However, selective mode excitation can improve only the short-haul MMF communication systems since mode mixing, resulting in cross-talk between modes, becomes significant as the length of the fiber increases. Instead of focusing only on the 3-dB modal band, the use of the multimode fiber's high-frequency region, which is higher than the 3-dB modal band, has been considered for bandwidth enhancement. It is found that as the frequency increases, the magnitude response of MMF does not decrease monotonically but becomes relatively flat at a particular level lower than the level at the 3-dB modal band [7]. In this high-frequency region, many passbands are available that can be used as channels in signal transmission. Additionally, the average bandwidth of each passband is approximately identical to the 3-dB modal bandwidth. However, these passbands are frequency-selective channels, meaning that the nulls in the response are numerous and vary from fiber to fiber. One technique that has been used to reduce the effect of frequency-selective fading channels is spread spectrum modulation, which is developed to increase the tolerance for signal transmission over frequency-selective fading channels. Direct Sequence Spread Spectrum (DSSS) [8]-[12], which is one kind of spread spectrum modulation, has been used to mitigate this issue. In DSSS, the original signal is multiplied with a known spread sequence, which covers a larger bandwidth than the original signal. The multiplication results in a wider bandwidth signal called the spread spectrum signal, in which the tolerance for the frequency-selective fading channel is added. To further improve the tolerance level, it has been suggested that a larger bandwidth spread sequence must be used, thus resulting in a larger required bandwidth for the spread spectrum signal. However, this approach then means that for a given MMF high-frequency bandwidth, the real data rate to be transmitted over this bandwidth is reduced. Additionally, as discussed previously, the bandwidth of each possible available passband in the high-frequency region of MMF approximately equals the 3-dB modal bandwidth. This

Manuscript received July 22, 2022; revised December 14, 2022; accepted December 29, 2022.
*Corresponding author email: surachetka@nu.ac.th

circumstance means that covering a larger bandwidth will also cover many possible nulls, which can further degrade the signal transmission.

One alternative technique that has been used to transmit a high data rate signal in the high-frequency region and lessen the signal degradation from nulls of MMF is Orthogonal Frequency Division Multiplexing (OFDM) [13]-[17]. In OFDM, multiple spaced orthogonal subcarrier signals with overlapping parallel narrow-band subcarriers are transmitted instead of a single wide band. Each spaced orthogonal subcarrier signal is sent by a lower data rate to maintain the total data rates as the rate sent by the conventional single-carrier modulation schemes. Unfortunately, the orthogonality between subcarriers of the OFDM system will be bothered by intercarrier interference (ICI) due to the high relative speed under rapidly time-varying multipath channels. One good choice to mitigate the effects of ICIs and reduce the effects of multiple nulls of MMF is subcarrier multiplexing (SCM). In SCM, the transmission signal is separated into multiple smaller data rate signals and then sent through the fiber using different subcarrier frequencies to avoid ICI and nulls of MMF. Applying the SCM to the high-frequency region of the MMF can help utilize the passbands effectively if the proper subcarrier frequencies, which are not located at or near any nulls, are known. In [18], the passbands at frequencies between 0.2 and 1.6 GHz or the low-frequency passbands have been studied and 6 available passbands are found. The middle frequency of each passband can be estimated. Using the estimated frequencies as subcarrier frequencies in SCM, the low-frequency passbands of MMF can then be used properly as channels for transmitting subcarrier signals. The performance of SCM transmission with MMF over these low-frequency passbands has been obtained [19], [20]. It is found that a total data rate of 500 Mbps with a Bit Error Rate (BER) lower than 10^{-6} can be obtained. It is also found that some low-frequency passbands can degrade the transmitted subcarrier signals. To lessen this effect, an error-correction code should be applied so that any errors affected by a particular passband can be corrected at the receiving end. There are two major classes of error-correction codes: convolution codes and block codes [21]. For convolution codes, any incorrect decoding process performed at the receiving end may result in catastrophic error propagation affecting the subsequent decoding process. On the other hand, for block codes, the original bits are divided into blocks, and each block is coded by adding extra bits to the block. The decoding process for any coded block is done independently from other coded blocks; hence, there is no catastrophic error if this coded block is decoded incorrectly. Linear block codes (LBCs) are one type of block code that can help correct any number of error bits depending on the design of the code. For example, (7, 4) LBC, in which each block contains 4 data bits and 3 extra bits, can correct any one-bit error at the destination. This (7, 4) LBC has been adopted with the SCM MMF system over low-frequency passbands [22] in hopes of lessening the effect of the null frequency at the passbands. A BER lower than 10^{-8} with a total data rate of 392 Mbps can be obtained. BER improvement can be achieved once LBC is implemented in the system.

Since DSSS needs a very large bandwidth for signal transmission and the ICI may be occurred while using OFDM technique for signal transmission in low-frequency regions. Many studies have shown that using SCM and LBC is a potential technique for high data rate signal transmission over MMF at low-frequency regions. SCM is used in utilizing the available low-frequency passbands of MMF as subcarrier channels. The total data rate obtained from the SCM MMF system is higher than the data rate gained only from the 3-dB modal band. The BER of the system is improved as LBC is applied. However, it is found that using LBC with one-bit error correction for data encoding may not be adequate to undo the errors introduced by some low-frequency passbands. Since the obtained BER is still 10^{-8}, which is too high to use in optical communication system. Therefore, using two-bit error correction code should be considered. Hence, it is interesting to view how the system performs if LBC with one-error-bit and two-error-bit correction codes are adopted with different types of bit allocation.

The purpose of this study is to determine the performance in terms of BER and data rate of a 1-km MMF SCM communication system. Different number of low-frequency passbands and different bit-allocations for LBC (whether one- or two-bit correction) are considered. Eventually, the BER versus data rate for different cases are summarized.

This work is presented as follows. An introduction has already been provided in Section I. Related theories, for example, handling low-frequency MMF response, linear block code, and the determination of the Q-parameter, are discussed in Section II. The communication system model and methodologies used in this work are described in Section III. In Section IV, the results of this work are shown and discussed. Finally, the findings in this work are summarized in Section V.

II. Related Theory

A. Low-Frequency Response of MMF

The frequency response of multimode fibers has previously been studied. Studies have shown that the MMF response depends on the delay of the guided mode in the fiber and can be determined as shown in Eq. (1) [23].

$$H_{fiber}(f) = \sum_{n=1}^{N_{\text{mode}}} e^{-j2\pi f t_{d,n}} \tag{1}$$

where $H_{fiber}(f)$ is the frequency response of MMF,

N_{mode} is the number of guided modes, and

$t_{d,n}$ is the delay time of the n^{th} mode, which can be modeled as a uniform random variable.

Eq. (1) shows the frequency response of MMF as the summation of N_{mode} exponential terms, each with different delay times. The delay times in Eq. (1) are defined

statistically as a uniform random variable with an average time delay of $t_{d,avg}$ and a deviation of $t_{d,dev}$. For example, if the length of MMF is 1 km, with $t_{d,avg}$ = 5 μs, $t_{d,dev}$ = 2.5 ns, and N_{mode} = 100 modes, then three frequency responses of the multimode fiber can be shown in Fig. 1. These three responses are from the three sets of delay times, $t_{d,n}$, which are randomly selected using a uniform distribution with the average and standard deviation, as mentioned earlier.

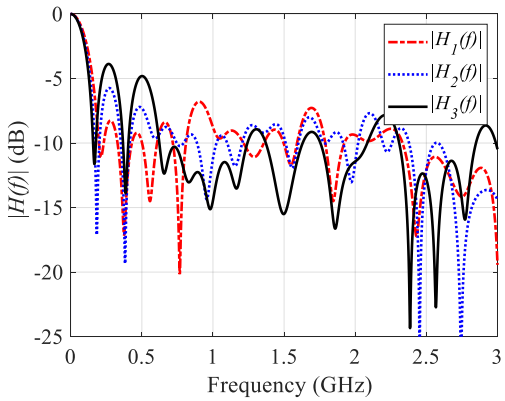

Fig. 1. Three MMF frequency response when N_{mode} = 100, $t_{d,avg}$ = 5 μs, and $t_{d,dev}$ = 2.5 ns.

Fig. 1 shows that many passbands are available at low frequencies from 0 - 1.6 GHz. The bandwidths for these passbands are very similar; that is, approximately 200 MHz, which is identical to the bandwidth of the 3-dB modal band at zero frequency. The three MMF low-frequency responses in Fig. 1 are very similar, and they occur from 0 to 200 MHz, which is referred to as the 3-dB modal bandwidth. Considering the frequency higher than 200 MHz shows that many passbands are available, and it has been studied that statistically, the bandwidth of these passbands is approximately identical to the 3-dB modal bandwidth. Hence, if these passbands are used as channels in signal transmission, the higher data rate in the MMF communication system can be increased. However, as seen from Fig. 1, passbands must be chosen carefully since the responses are frequency-selective and vary from fiber to fiber. The optimal frequencies between 0 to 1.6 GHz have been previously analyzed [17], and seven useful passbands have been identified. One of these frequencies is inside the 3-dB modal band, and the other six are low-frequency passbands beyond the 3-dB modal band. Within each of these seven passbands, the most efficient peak frequencies $f_{peak,avg}$ (i) in GHz units for use as subcarrier frequencies are found as follows in Eq. (2):

$$f_{peak,avg}(i) = \begin{cases} 0 & ;\ i = 0 \\ \dfrac{1.305i + 0.0298}{2t_{d,dev}} & ;\ i = 1, 2, \ldots, 6 \end{cases} \quad (2)$$

where i is the i^{th}-passband.

Eq. (2) shows how subcarrier frequencies have been determined for the seven low-frequency passbands. The first one (for i = 0 in Eq. (2)) is a 3-dB modal bandwidth, and the other six are low-frequency passbands (for i = 1 to 6). Using Eq. (2) with $t_{d,dev}$ = 2.5 ns, the $f_{peak,avg}$ values for passband #0 to passband #6 can be determined, that is, at 0, 267, 528, 789, 1,050, 1,311, and 1,572 MHz. Comparing these calculated $f_{peak,avg}$ values to the corresponding simulated $f_{peak,avg}$ values, the errors in percentages are determined and shown in Fig. 2 [17].

Fig. 2 shows that Eq. (2) can be used to estimate $f_{peak,avg}$ for low-frequency passbands, with all error rates lower than 4%, except for passband #1, where the error rate is 7.18%. However, a better formula specifically developed for determining $f_{peak,avg}$ for passband #1 calculated this value as 300 MHz [18]. This leaves a revised list of $f_{peak,avg}$ values for passbands #0 to #6 of 0, 300, 528, 789, 1,050, 1,311, and 1,572 MHz. These $f_{peak,avg}$ values for passbands #0 to #6 have been used in MMF communication systems [18], [19], [21] to study the performance of the low-frequency passbands. The results show that some of these passbands are affected by the null MMF response. This effect can be reduced using linear block code [21].

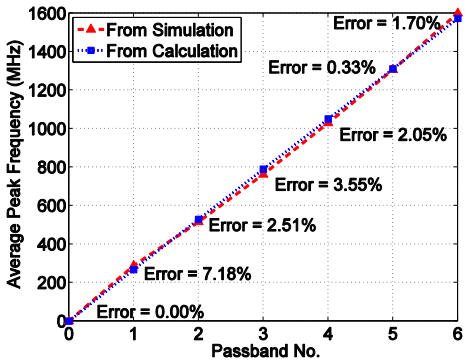

Fig. 2. Comparing estimated and simulated $f_{peak,avg}$ values [17].

B. Linear Block Code

Although the encoding of data is an effective methodology for increasing the performance of communication systems, using encoded data adds complexity to a communication system, and the transmission rate decreases, so choosing the appropriate type of encoding is crucial. One common type of encoding used in communication systems is forward error correction (FEC). FEC is used to correct error bits at the signal destination without requesting retransmission from the transmitting end. Two major kinds of systematic FEC are used: convolutional code and linear block code (LBC) [23], [24]. These two kinds of codes use the original message bits as the input for generating the parity check bits, which will be appended to the input message bits forming coded bits. One major difference between these two kinds of FECs is the memory requirement. The convolutional code requires memories in the coding process, while LBC does not. For LBC, a sample model with k-input message bits and n-output encoded bits is shown in Fig. 3.

Fig. 3 shows how the original message bits are divided into blocks of k bits, which are represented as matrix **m** in Eq. (3). Then, each k-bit block produces the encoded n bits, which are represented as matrix **c** in Eq. (3). The n bits consist of the original k bits and (n – k) parity bits. The

number of error bits that can be corrected depends on the number of parity bits. The encoded matrix **c** is determined by multiplying the vector **m** and the generator matrix **G**, as shown in Eq. (3) [25].

$$\mathbf{c} = \mathbf{mG} = \left[m_0, m_1, ..., m_{k-1}\right] \begin{bmatrix} g_{0,0} & g_{0,1} & \text{L} & g_{0,n-1} \\ g_{1,0} & g_{1,1} & \text{L} & g_{1,n-1} \\ \text{M} & \text{M} & \text{O} & \text{M} \\ g_{k-1,0} & g_{k-1,1} & \text{L} & g_{k-1,n-1} \end{bmatrix} \quad (3)$$

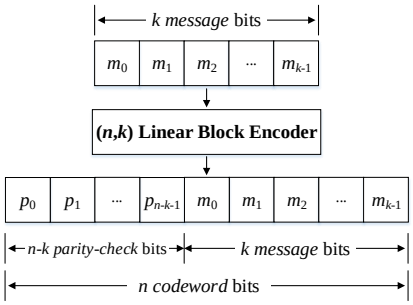

Fig. 3. Model of the (*n*, *k*) linear block code.

Eq. (3) shows how linear block codes are generally defined by two parameters: *n* and *k*. These two values are used to identify any given linear block code. Many kinds of linear block codes are available, including one-bit error correction, for example, (7, 4), (15, 11) and (31, 26), and two-bit error correction, for example, (15, 7) and (31, 21). In the case of (7, 4), (15, 11), (15, 7) and (31, 26) linear block codes, the generator matrix **G** can be determined using the respective generator polynomials [25]: $g(x) = x^3 + x + 1$, $g(x) = x^4 + x + 1$, $g(x) = x^8 + x^7 + x^6 + x^4 + 1$ and $g(x) = x^{10} + x^9 + x^8 + x^6 + x^5 + x^3 + 1$, respectively. An LBC with a relatively high *k*/*n* ratio is considered a "high code rate" LBC. One can see that the higher the code rate of a given LBC, the more complicated its generator matrix **G** will be.

C. Q-Parameter

The effectiveness of digital communication systems is often measured with the bit error rate (BER) parameter. This parameter can be described as the probability that bit error can occur at the signal destination. Normally, the minimum required BER for the optical communication system is lower than 10^{-9}. The Q-parameter is a semi analytical technique that can be applied to a communication system to evaluate its BER. For example, the Q-parameter will be an important factor when calculating the BER of an amplitude shift keying (ASK) transmission. In an ASK transmission, when sending binary data, there are 2 amplitudes representing bit 0 and bit 1. If bit 0 is represented by amplitude = 0 and bit 1 is represented by amplitude = 1, then ASK transmission will be referred to as on-off keying (OOK). Noted that OOK is indeed intensity modulation, which is the modulation technique commonly used in optical communication system. Additionally, utilizing this type of modulation, the phase noise caused by different delays from different guided modes of the multimode fiber cannot affect the system performance. When a signal arrives at the destination, the communication system needs to first look at the signal as a whole and define the "decision threshold" ($I_{threshold}$), above which a bit will be considered bit 1 and below which it will be considered bit 0. In preparation for determining the decision threshold, the communication system first calculates the respective average amplitudes of the received signals for bit 0 and bit 1 (that is, μ_0 and μ_1, respectively) and the corresponding standard deviations (that is, σ_0 and σ_1, respectively), as shown in Fig. 4.

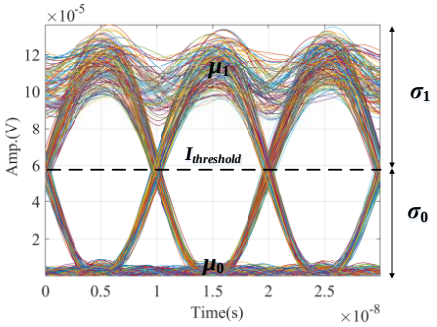

Fig. 4. Eye pattern from the received signal and average amplitudes for bit 0 and bit 1.

With the average amplitudes and standard deviations of bit 1 and bit 0 in hand, the decision threshold ($I_{threshold}$) can be determined with Eq. (4) [7]:

$$I_{threshold} = \frac{\sigma_0 \mu_1 + \sigma_1 \mu_0}{\sigma_0 + \sigma_1} \quad (4)$$

The average amplitudes and standard deviations can also be used to calculate the BER for this OOK transmission, as shown in Eq. (5) [19]:

$$BER_{OOK} = K\left(\frac{\mu_1 - \mu_0}{\sigma_1 + \sigma_0}\right) = K(x) \quad (5)$$

where μ_0 = the average amplitude of the received bit 0 signal,
μ_1 = the average amplitude of the received bit 1 signal,
σ_0 = the standard deviation of the received bit 0 Signal,
σ_1 = the standard deviation of the received bit 1 Signal,
$K(x)$ is the probability that a zero-mean unit-variance Gaussian random variable exceeds *x*.

From the discussion done in this section, it is seen that low-frequency passbands of MMFs can be used as channels for an SCM system, as shown in Fig.1, in order to increase the total data rate of an MMF communication system. Carefully selection of peak frequencies for each passband suggested in [18] is useful since it can reduce the opportunity of null-frequency selection. In this work, the related theory about MMFs and peak-frequency selection

is applied. To further reduce the obtained BER, linear block codes with different numbers of bit-error correction are studied. Additionally, different sets of low-frequency passbands to be used as sub-channels are considered. The results from the study should provide an insightful performance in terms of BER and data rates of an MMF communication system using low-frequency passbands with linear block codes.

III. Methodology

In this section, the methodology for the study is described. The diagram explaining the scope of this work is shown in Fig. 5.

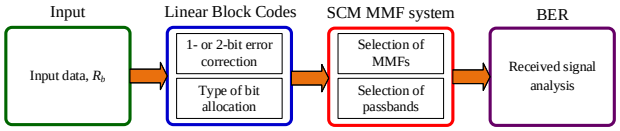

Fig. 5. Diagram for the study.

From Fig. 5, it is seen that there are four major parts involved in this study. The first part is the input data, in which the data rate of R_b is considered. Next, the input data will be encoded using linear block codes. The number of error bits to be corrected and type of bit-allocation to be used are selected. The explanation about bit-allocation is given in Part *C* of this section. The encoded bits are then sent to the SCM MMF communication system. At this part, 5 MMFs will be used and different selections of low-frequency passbands are studied. The selected 5 MMFs are explained in Part *B*. The received signal will be analyzed and the BER will be evaluated. BER determination for different types of LBCs and bit-allocation types is shown in Part *D*.

A. Optical Communication System with SCM

Now, a multimode fiber communication system using subcarrier multiplexing (SCM) and linear block code will be described. The communication model developed for the current study is shown in Fig. 6.

Fig. 6 shows how the input data bits are generated at the "Bit Gen" block with a total data rate of R_b. These data bits are sent to a block encoder to generate the coded output bits. The bit rate of the output is thus increased to $R_{b,coded}$, which depends on the kind of linear block code used. These coded bits are sent to a serial-to-parallel block to separate the coded bits into many paths (7 paths, as seen from the figure). The coded data for each path are sent to "Pulse Gen" to generate Gaussian pulses if the coded data are bit 1; otherwise, the output signal will be zero. This signal is then sent to the corresponding ASK generator to create that path's ASK signal. Each signal is then forwarded to its assigned modulator. The seven subcarrier frequencies in this work are represented as $f_{sub,0}$; $f_{sub,1}$; $f_{sub,2}$; $f_{sub,3}$; $f_{sub,4}$; $f_{sub,5}$; and $f_{sub,6}$, which are at 0, 300, 528, 789, 1,050, 1,311, and 1,572 MHz, respectively. The prepared subcarrier signals are then bundled and moved to the laser, where they are converted from an electrical signal to a light signal. Now, the light signal is transmitted over the multimode fiber with $t_{d,avg}$ = 5 μs, $t_{d,dev}$ = 2.5 ns, N_{mode} = 100 modes, and a fiber length of 1 km. At the signal destination, the received light signal is detected by the photodetector, which is mathematically modeled as a square-law detector (assuming that PIN detector and transimpedance amplifier receiver are used). Then, the received light signal is transformed into the received electrical signal. Thermal noise is added to the received electrical signal. The received electrical signal is sent to 7 bandpass filters. Each filtered signal is demodulated and low-pass filtered back to its baseband signal. Each demodulated signal is sent to the decision circuit to identify each received output bit as either 0 or 1. The seven output bitstreams then meet again at the parallel-to-serial block, where they are once more combined and sent onward at a total data rate of $R_{b,coded}$. Finally, the combined output bits are sent to a decoder block to correct any errors that occurred during transmission. The data rate and BER of this optical system are measured to evaluate its performance.

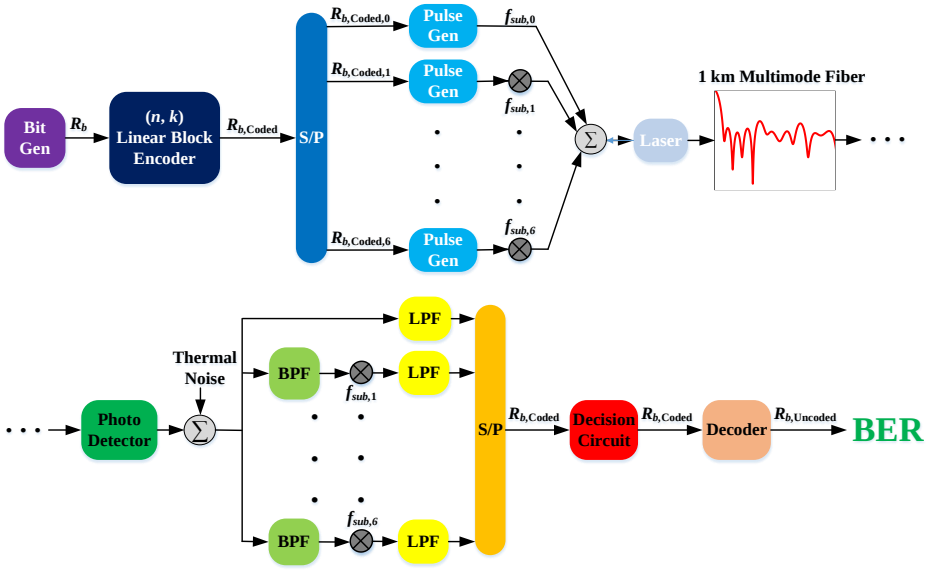

Fig. 6. This study's multimode fiber communication model.

B. Selecting Multimode Fibers for the Study

This study uses five MMFs for all tests, and since variation in individual fiber performance occurs naturally, the five fibers used need to realistically represent that variation. Therefore, ten MMFs will initially be tested for individual BER performance, and then based on the results, the five fibers for use in this study will be selected in the following way. First, the two fibers with the highest BERs will be selected for use. Next, the two fibers with the lowest BERs will also be selected for use. Finally, the average of the six remaining fibers' BERs will be calculated, and the fiber from those six that is closest to that average BER will be the final fiber selected. To this end, each of the ten initial MMFs was tested using the model shown in Fig. 6, except that neither the linear block encoder nor the linear block decoder was used. A random bit signal was transmitted with a total data rate of 800 Mbps sent over the MMF with the 7 low-frequency channels specified earlier (passbands #0 to #6, ranging in frequency from 0 to 1.6 GHz). The total data rate of 800 Mbps was divided between the seven channels, with a data rate of 200 Mbps transmitted over passband #0 (the 3-dB modal bandwidth) and 100 Mbps transmitted over each of the other 6 passbands (passbands #1 to #6). This study was then repeated using three other total data rates: 600, 400, and 300 Mbps. Similarly, each of these lower total data rates was allocated into the seven passbands using the same earlier proportions. Thus, there were 40 tests (10 fibers × 4 data rates). All the BER results are shown in Fig. 7, where they are grouped by data rate.

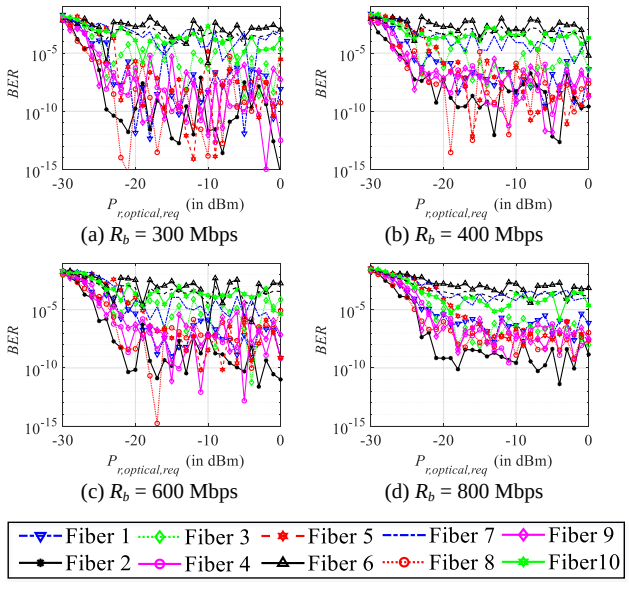

Fig. 7. The 10 BER curves for each of the 4 data rates.

The BER curves from the 10 MMFs with data rates of 300, 400, 600 and 800 Mbps in Fig. 7(a), 7(b), 7(c) and 7(d), respectively, show that when the received optical power is increased, the obtained BERs decrease. Looking at Fig. 7(a), when the received optical power ($P_{r,optical,req}$) is higher than -15 dBm, the lowest BER curves are Fiber #2 and Fiber #8, which are lower than 10^{-7}, while the highest BER curves are Fiber #6 and Fiber #10. The other BER curves are distributed between these highs and lows. In all three remaining data rates, the highest and lowest BER curves are the same as in Fig. 7(a). Therefore, using the fiber selection criteria explained above, the 5 MMFs used in this study are Fiber #2, Fiber #6, Fiber #8, Fiber #9 and Fiber #10, which will hereafter be referred to as Fiber A, Fiber B, Fiber C, Fiber D and Fiber E, respectively.

C. Bit Allocation

As mentioned earlier, 7 low-frequency passbands (passbands #0 to #6) are used as a channel for sending the encoded signal in the form of linear block code. The encoded bit allocation of each passband is shown in Fig. 8. Since the transmission capacity of passband #0 is twice that of any of the other six passbands, passband #0 appears twice in Fig. 8.

In Fig. 8, each block of the (7, 4) LBC consists of 7 bits: 3 parity bits (p_0, p_1, and p_2) and 4 message bits (m_0, m_1, m_2, and m_3). Two bits are allocated to passband #0 (the 3-dB modal bandwidth), and one bit is allocated to each of the other 6 passbands. In the first block, shown in the first seven hatched squares under the passband labels, bits p_0 and p_1 are transmitted over passband #0, followed by bits p_2, m_0, m_1, m_2 and m_3, transmitted over passbands #1 to #5, respectively. Since passband #6 was not used for sending the first block, the second block transmission will start at passband #6. Therefore, in the second block, bit p_0 is transmitted over passband #6, followed by bits p_1, p_2, m_0, m_1, m_2 and m_3, which are transmitted over passbands #0 to #4, respectively. This sequence is repeated for a total of eight blocks, forming seven rows in Fig. 8, before these seven rows simply start over again. In this way, the parity bits are distributed across every available slot of every available passband, leaving no slot vacant and making most of the available bandwidth. However, using linear block codes other than (7, 4) will require a different allocation of bits. The other LBCs used in this study are (15, 11), (15, 7), (31, 26), and (31, 21) LBC. The bit allocations for transmitting (15, 11) and (15, 7) LBC are shown in Fig. 9.

Passband							
#0	#0	#1	#2	#3	#4	#5	#6
p_0	p_1	p_2	m_0	m_1	m_2	m_3	p_0
p_1	p_2	m_0	m_1	m_2	m_3	p_0	p_1
p_2	m_0	m_1	m_2	m_3	p_0	p_1	p_2
m_0	m_1	m_2	m_3	p_0	p_1	p_2	m_0
m_1	m_2	m_3	p_0	p_1	p_2	m_0	m_1
m_2	m_3	p_0	p_1	p_2	m_0	m_1	m_2
m_3	p_0	p_1	p_2	m_0	m_1	m_2	m_3

p_i Parity bits

m_i Message bits

Fig. 8. Bit allocation for this study's (7, 4) LBC transmission.

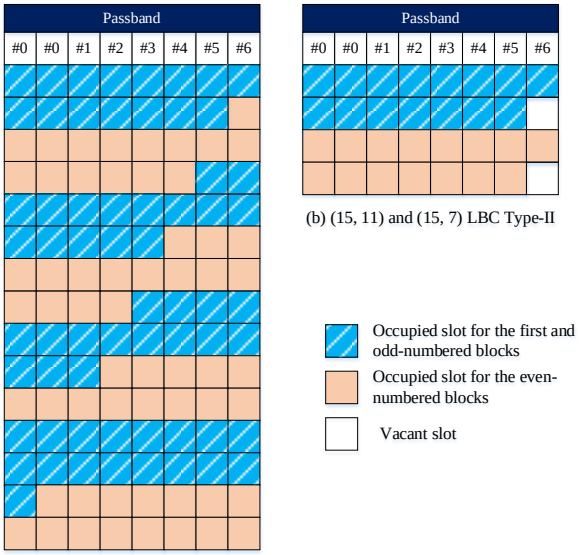

(a) (15, 11) and (15, 7) LBC Type-I

(b) (15, 11) and (15, 7) LBC Type-II

Fig. 9. Bit allocation for (15, 11) and (15, 7) LBCs.

In Fig. 9, (15, 11) LBC and (15, 7) LBC have a similar bit-allocation pattern, and bits can be allocated into the slots in two ways, referred to as Type-I and Type-II. In Type-I, all slots are assigned encoded bits, without leaving any slot vacant. The bit-allocation pattern is repeated every eight blocks of encoded bits. In this first type of bit allocation, each passband is fully utilized, wasting no bandwidth and resulting in a high transmission rate. However, if attenuation occurs in any passband in Type-I, multiple error bits may be received at the destination. On the other hand, Type-II bit allocation in Fig. 9(b) is not a set of eight repeating blocks but rather a single block repeating over and over, and that block always has one vacant slot in passband #6, since all 15 encoded bits are already assigned. The data rate of Type-II bit allocation is slightly lower than that in Type-I (because of that one unoccupied slot). However, if any attenuation occurs in passband #6, it will cause fewer error bits because an empty slot contains no data that can be corrupted. Because of its potentially lower error rate, Type II may result in a lower BER than Type I. Although not shown explicitly here, the bit-allocation patterns of (31, 26) LBC and (31, 21) LBC are very similar to Fig. 9, again each having a Type-I allocation of 8 repeating blocks and a Type-II allocation of a single repeating block.

D. BER Determination

As mentioned earlier, the BER of any OOK signal transmission can be calculated using Eq. (5). For example, in the case of the (15, 11) linear block code Type-I shown in Fig. 9(a), two bits are assigned to passband #0, and one bit is assigned to each of the other six passbands. This bit-allocation pattern is repeated every eight blocks of encoded bits. The probability of there being no error during transmission of this 15-bit block over the multimode fiber can be calculated as follows:

$$P[\text{no error}]_{\text{Type-I}} = \frac{\sum_{l=1}^{m}\left(\prod_{j=1}^{n}(1-p_j)\right)}{m} \tag{6}$$

where p_j is the probability of a bit error occurring in the j^{th} bit,

n is the number of encoded bits in a single block; in this case, 15,

m is the number of repetitions of the full bit-allocation pattern, in this case, 8.

which yields:

$$P[\text{no error}]_{\text{Type-I}} = \frac{\sum_{l=1}^{8}\left(\prod_{j=1}^{15}(1-p_j)\right)}{8} \tag{7}$$

Since the (15, 11) linear block code can correct one-bit error per 15-bit block transmission at the signal destination, then the probability of having a one-bit error is as follows:

$$P[\text{1-bit error}]_{\text{Type-I}} = \frac{\sum_{l=1}^{m}\left[\sum_{j=1}^{n}\left(\left[\prod_{i=1,i\neq j}^{n}(1-p_i)\right]\times p_j\right)\right]}{m} \tag{8}$$

where p_i is the probability of a one-bit error occurring in the i^{th} bit.

$$P[\text{1-bit error}]_{\text{Type-I}} = \frac{\sum_{l=1}^{8}\left[\sum_{j=1}^{15}\left(\left[\prod_{i=1,i\neq j}^{15}(1-p_i)\right]\times p_j\right)\right]}{8} \tag{9}$$

Using Eq. (7) and (8), the system BER can then be calculated as follows:

$$BER_{\text{Type-I}} = \frac{1-P[\text{no error}]_{\text{Type I}} - P[\text{1-bit error}]_{\text{Type I}}}{n} \tag{10}$$

Thus,

$$BER_{\text{Type-I}} = \frac{1-P[\text{no error}]_{\text{Type I}} - P[\text{1-bit error}]_{\text{Type I}}}{15} \tag{11}$$

Eq. (11) shows that the probability of a wrong decision (i.e., an error bit) in a received 15-bit block is the complement of the combined probabilities of no error and one-bit error divided by 15. A similar calculation can be used to obtain the system BER for Type-II bit allocation. The calculation will be less complex since in Type-II bit allocation, only a single block is repeated over and over during transmission of the encoded bits via the multimode fiber. However, a (15, 7) linear block code can correct two-bit errors per 15-bit block transmission at the signal destination. To find the BER in this case, one needs three things: the probability of no error occurring during transmission of the 15-bit block, the probability of having a single bit error, and the probability of having two-bit errors. The probability of having two-bit errors can be calculated as follows:

$$P[\text{2-bit error}]_{\text{Type-I}} = \frac{\sum_{l=1}^{m}\left[\sum_{j=1}^{n}\left(\left[\prod_{i=1,i\neq j\neq k}^{n}(1-p_i)\right]\times p_j\times p_k\right)\right]}{m} \tag{12}$$

where p_k is the probability of a bit error occurring in the k^{th} bit.

Thus,

$$P[\text{2-bit error}]_{\text{Type-I}} = \frac{\sum_{l=1}^{8}\left[\sum_{j=1}^{15}\left(\left[\prod_{i=1,i\neq j\neq k}^{15}(1-p_i)\right]\times p_j \times p_k\right)\right]}{8} \quad (13)$$

The system BER of the (15, 7) linear block code can then be determined as follows:

$$BER_{\text{Type-I}} = \frac{\left[\begin{array}{l}1-P[\text{no error}]_{\text{Type I}}\\ -P[\text{1-bit error}]_{\text{Type I}}\\ -P[\text{2-bit error}]_{\text{Type I}}\end{array}\right]}{15} \quad (14)$$

Note that a similar calculation can be done to find the system BER of any linear block code having a Type-II bit allocation and two-bit error correction.

IV. Results and Discussion

In this section, the performance in terms of BER for different transmission settings is studied. These settings are from different number of low-frequency passbands used in the transmission; that is, 6, 5, and 4 low-frequency passbands. Note that, for each setting, different number of error bits to be corrected by LBC and different types of bit allocation are applied in order to compare the obtained BERs. Additionally, in the last part, the maximum data rate and BER estimation is shown and discussed.

A. Simulation of MMF Communication with a 3-dB Modal Band and 6 Low-Frequency Passbands

In this section, five types of linear block code were sent at a high transmission rate over an optical communication system, as shown in Fig. 6, with five multimode fibers referred to as Fibers A, B, C, D, and E. The performance of this communication system can be measured in terms of BER curves, as shown in Fig. 10.

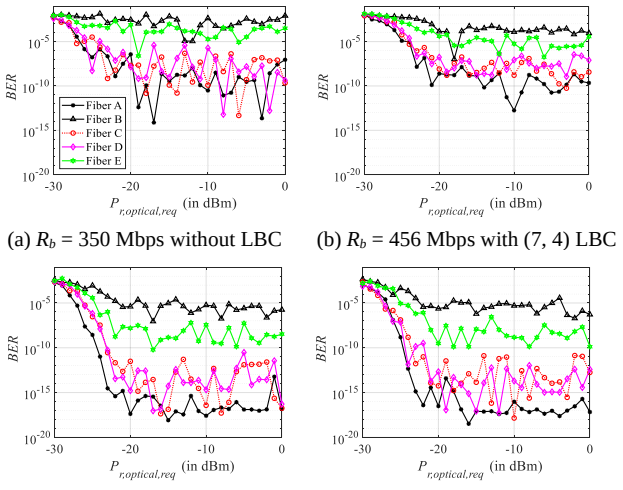

(a) R_b = 350 Mbps without LBC (b) R_b = 456 Mbps with (7, 4) LBC

(c) R_b = 583 Mbps with (15, 11) LBC and Type-I (d) R_b = 550 Mbps with (15, 11) LBC and Type-II

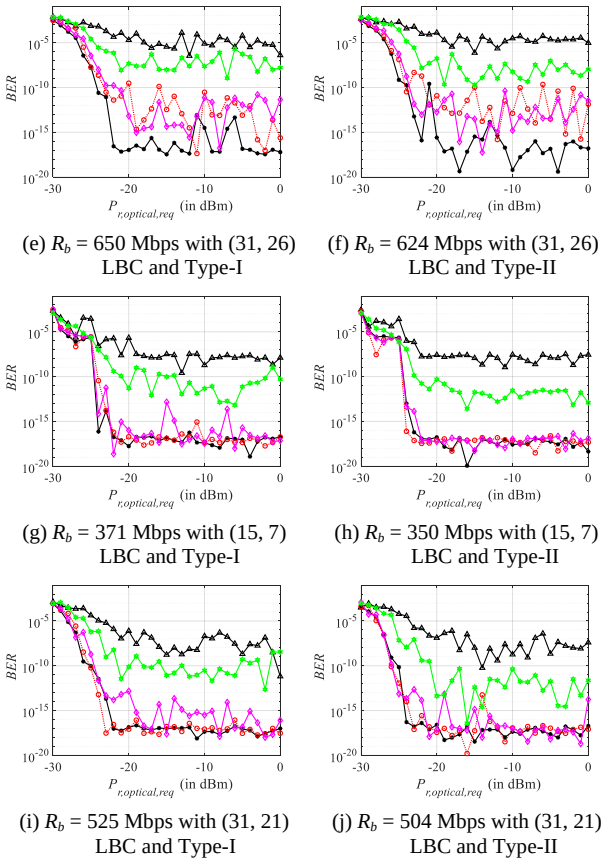

(e) R_b = 650 Mbps with (31, 26) LBC and Type-I (f) R_b = 624 Mbps with (31, 26) LBC and Type-II

(g) R_b = 371 Mbps with (15, 7) LBC and Type-I (h) R_b = 350 Mbps with (15, 7) LBC and Type-II

(i) R_b = 525 Mbps with (31, 21) LBC and Type-I (j) R_b = 504 Mbps with (31, 21) LBC and Type-II

Fig. 10. BERs of 10 combinations of LBC and bit allocation when using the 3-dB modal band and 6 low-frequency passbands.

Fig. 10 shows the BER curves resulting from 10 combinations of LBC and bit allocation sent over an MMF communication system having a 3-dB modal band and 6 low-frequency passbands (passband #1 to passband #6). The data rates obtained from these 10 cases are also shown separately in Fig. 11. Fig. 10(a) shows what happens when the data rate of 350 Mbps is sent over the MMFs without any linear block code. This data rate was chosen for use as a reference. When the received optical power ($P_{r,optical,req}$) is higher than -15 dBm, the BER curves vary from 10^{-14} to 10^{-2}, which is a very wide range. The highest (worst) BER curve at 10^{-2} came from Fiber B, and 10^{-2} is definitely too high to use in an optical communication system.

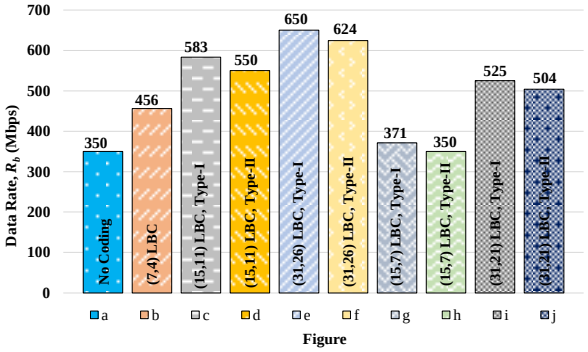

Fig. 11. Data rate of 10 combinations of LBC and bit allocation when using the 3-dB modal band and 6 low-frequency passbands.

Fig. 10(b) shows the BER curves when using the transmission rate of 798 Mbps with (7, 4) LBC. The resulting data rate is 456 Mbps, and this type of linear block code can correct a one-bit error at the signal destination. When the received optical power ($P_{r,optical,req}$) is higher than -15 dBm, the BER curves vary from 10^{-13} to 10^{-3}, and Fiber B still has the highest BER curve at 10^{-4}. The BER curves in this case are slightly lower than those in Fig. 10(a), yet the data rate in this case increases to 456 Mbps. Note that the variation in the obtained BERs from this figure is clearly less than that from Fig. 10(a).

Figs. 10(c) and 10(d) use (15, 11) LBC (at transmission rates of 795 Mbps and 750 Mbps, respectively), so both can correct the one-bit error each at the signal destination, similar to the previous case in Fig. 10(b). However, the code rate in these two cases is higher, which leads to a higher data rate than in Fig. 10(b). Comparing Fig. 10(c) and Fig. 10(d), their respective data rates are 583 Mbps and 550 Mbps. Fig. 10(c)'s data rate is higher because it uses Type-I bit allocation, as shown earlier in Fig. 9(a), so all slots are assigned encoded bits, without leaving any slot vacant. Since each passband is fully utilized, no bandwidth is wasted, and the transmission rate is higher. On the other hand, Fig. 10(d) uses Type-II bit allocation, as shown earlier in Fig. 9(b), and since a vacant slot is left in passband #6, the transmitted data rate is not quite as high as in Fig. 10(c). However, the resulting BER curves in Fig. 10(c) and Fig. 10(d) are very similar. When the received optical power ($P_{r,optical,req}$) is above -15 dBm, Fiber B still has the highest BER in Fig. 10(c) and 10(d). The other BER curves in both figures vary between 10^{-18} and 10^{-7}; therefore, both of these cases are potentially useable in an optical communication system.

Fig. 10(e) and Fig. 10(f) use (31, 26) LBC, but Fig. 10(e) uses Type-I bit allocation, while Fig. 10(f) uses Type-II bit allocation. As in the previous three cases, Fig. 10(e) and 10(f) can correct a one-bit error each at the signal destination. However, their code rate is higher, which yields data rates of 650 Mbps and 624 Mbps, respectively. When the received optical power ($P_{r,optical,req}$) is above -15 dBm. Fiber B still has the highest BER in Fig. 10(e) and Fig. 10(f) at 10^{-4}. However, for the other BER curves, it is seen that the resulting BERs from Fig. 10(f), which vary between 10^{-19} and 10^{-7}, are better than those from Fig. 10(e), which vary between 10^{-18} and 10^{-6}.

All four of the remaining cases in Fig. 10 can correct two-bit errors each. Fig. 10(g) and 10(h) use (15, 7) LBC. The data rate for Fig. 10(g) was 371 Mbps, and the data rate for Fig. 10(h) was 350 Mbps. The data rate in these two cases is the lowest because they have the lowest code rate ratio, which is 7/15 (= 0.47). When the received optical power ($P_{r,optical,req}$) is higher than -15 dBm, Fiber B still has the highest BER in these two cases at 10^{-7}, and the other BER curves are lower than 10^{-9}. The results in Figs. 10(g) and 10(h) have lower BER curves than any of the previous cases thus far, lower even the case of using the data rate of 350 Mbps without any LBC in Fig. 10(a).

Fig. 10(i) and Fig. 10(j) show the BER curves when using (31, 21) LBC Type-I and Type-II bit allocations, respectively. This kind of linear block code can correct the two-bit errors at the signal destination, as in Fig. 10(g) and Fig. 9(h), but the code rates in Fig. 10(i) and Fig. 10(j) are higher (that is, 21/31 = 0.68), yielding data rates for both cases of 525 and 504 Mbps, respectively. When the received optical power ($P_{r,optical,req}$) is higher than -15 dBm, Fiber B still has the highest BER at $10^{-6,}$ and the other BER curves are all lower than 10^{-9}, so the other fibers could still theoretically be used in an optical communication system.

Now, if within each Fig. 10(a) through 10(j), the BER curves of the five fibers are averaged together, then those 10 averages can be seen in Fig. 12. One can see that the BER curves in Fig. 12 appear in three main groups, labeled Groups **a**, **b**, and **c**. Recall that Group **a** is the only BER curve using the data rate of 350 Mbps without any linear block code. When the received optical power ($P_{r,optical,req}$) is higher than -15 dBm, the BER curve is higher than 10^{-3}. Five BER curves are in Group **b**, and when the received optical power ($P_{r,optical,req}$) is higher than -15 dBm, these curves vary from 10^{-7} to 10^{-5}. The five BER curves in Group **b** originate from the cases using (7, 4) LBC; (15, 11) LBC Type-I; (15, 11) LBC Type-II; (31, 26) LBC Type-I; and (31, 26) LBC Type-II, and all five can correct one-bit error each at the signal destination. The maximum data rate of Group **b** is 650 Mbps, which comes from the case of (31, 26) LBC Type-I bit allocation. The lowest data rate of Group **b** is 456 Mbps, which comes from the case using (7, 4) LBC. All the BER curves in Group **b** are clearly lower than the BER curve in Group **a**. This result demonstrates the higher performance gained by using linear block code in an MMF communication system.

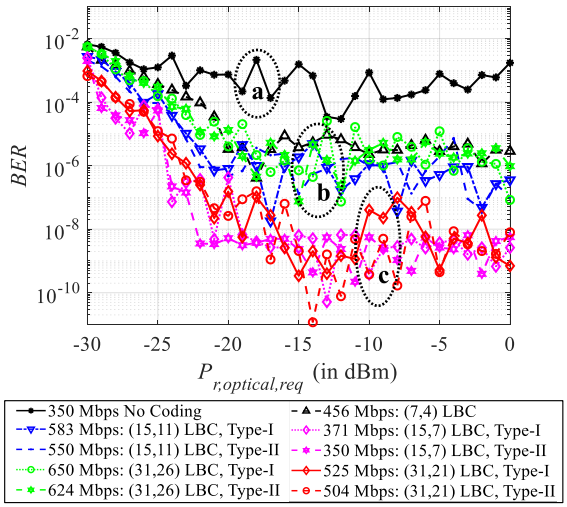

Fig. 12. Data rate of 10 combinations of LBC and bit allocation when using the 3-dB modal band and 6 low-frequency passbands.

Considering Group **c** in Fig. 12, four BER curves are presented using (15, 7) LBC Type-I; (15, 7) LBC Type-II; (31, 21) LBC Type-I; and (31, 21) LBC Type-II, each of which can correct two-bit error at the signal destination. When the received optical power ($P_{r,optical,req}$) is higher than -15 dBm, the four BER curves vary from 10^{-11} to 10^{-7}. The

maximum data rate sent in this group is 525 Mbps, which comes from the two cases of using (31, 21) LBC Type-I bit allocation. Comparing these three groups, the highest BER comes from Group **a,** and the lowest BERs come from Group **c**. Group **c** has the lowest BER curves because of the performance gained by two-bit error correction. If the minimum requirement of a particular communication system is a BER lower than 10^{-7}, Fig. 12 shows that Group **a** and Group **b** cannot satisfy that requirement but that only Group **c** can. The BER curves in Groups **b** and **c** are clearly lower than the BER curve in Group **a**. These results confirm the benefits of using linear block code.

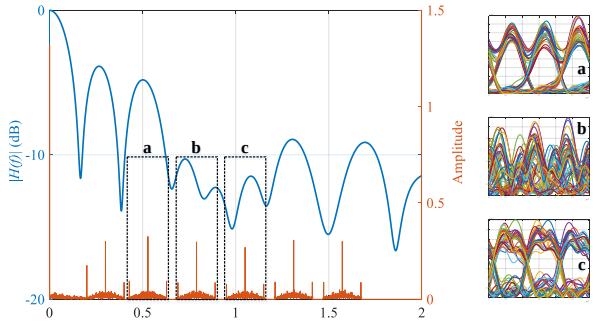

Fig. 13. The frequency response of Fiber B is shown together with the subcarrier frequency components.

One result that clearly stands out from Fig. 10 is that Fiber B has the highest BER curve of the ten cases. To lessen the issues that lead to a very high BER, it is helpful to take a closer look at the frequency response of Fiber B and at the seven frequency components of the transmitted subcarrier signal. These are all shown in Fig. 13.

As mentioned earlier, the author of [18] found that BERs from passbands #2 to #4 are very high. Fig. 13 shows the eye patterns of the received signals from those three passbands. Looking at eye patterns **a** and **c** (from the received signal of passbands #2 and #4, respectively), it is easy to distinguish between bit 0 and bit 1 in these two eye patterns. The main frequency component locations used in Fig. 13 for passbands #2 and #4 work well in case Fiber B. However, looking at eye pattern **b**, it is almost fully closed, with bit 0 and bit 1 being virtually indistinguishable, leading to a very high BER for passband #3. This is the result of the main frequency component of subcarrier #3 being located at the null of its channel. Therefore, in this case, passband #3 is not a good candidate channel for this particular communication system. The performance of the system without using passband #3 will be given next.

B. Simulation of MMF Communication with a 3-dB Modal Band and 5 Low-Frequency Passbands

In this next MMF communication system simulation, passband #3 was not used as a channel. The simulation results from using the 3-dB modal band and 5 low-frequency passbands (passbands #0, #1, #2, #4, #5 and #6) are shown in Fig. 14.

Fig. 14(a) and Fig. 14(b) show the BER curves when six low-frequency passbands are used as a channel in MMF communication with (31, 21) LBC Type-I and Type-II, respectively. In Fig. 14(a), the data rate was 462 Mbps (corresponding to a transmission rate of 682 Mbps). In Fig. 14(a), when the received optical power ($P_{r,optical,req}$) is higher than -15 dBm, the BER curve from Fiber B is lower than 10^{-16}, verifying that Fiber B is indeed improved by not using passband #3 in the MMF communication. The other BER curves vary between 10^{-18} and 10^{-14}, except for the BER curve from Fiber E, which is the highest BER, but which is still lower than 10^{-9}, the upper limit for MMF communication systems. In Fig. 14(b), the data rate was 420 Mbps (with a transmission rate of 620 Mbps). Similarly, Fiber B is improved, and when the received optical power ($P_{r,optical,req}$) is higher than -15 dBm, all of the BER curves vary between 10^{-18} and 10^{-15}, except for the BER curve from Fiber E, which has the highest BER, although it is still lower than 10^{-10}. Hence, the data rate in Fig. 14(b) is lower than that in Fig. 14(a), and the BER curves in Fig. 14(b) are slightly lower than those in Fig. 14(a) because of the use of Type-II bit allocation. Considering Fig. 10(i) and Fig. 14(a), which represent the BERs when using (31, 21) LBC and Type-I, and Fig. 10(j) and Fig. 14(b), which represent the BERs when using (31, 21) LBC and Type-II, Fiber B's BER curves in Fig. 14(a) and 14(b) are significantly lower than Fiber B's BER curves in Fig. 10(i) and Fig. 10(j). However, the transmitted data rate in Fig. 14(a) and Fig. 14(b) decreases to 462 and 420 Mbps, respectively, because of the reduced number of channels used in this system (since passband #3 was not used in Fig. 14).

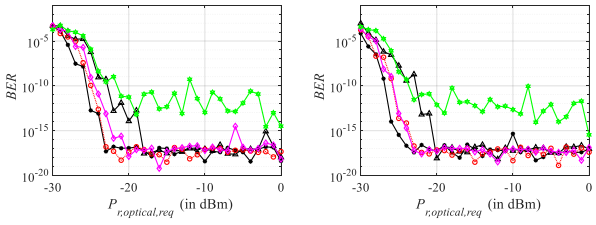

(a) R_b = 462 Mbps with (31, 21) LBC and Type-I

(b) R_b = 420 Mbps with (31, 21) LBC and Type-II

Fig. 14. BERs of (31, 21) LBC with the two types of bit allocation when using the 3-dB modal band and 5 low-frequency passbands.

Similar to Fig. 12, averaging the five BER curves in each of the ten combinations of LBC and bit allocation (since all ten combinations were tested, even though only the two best results are shown in Fig. 14), the results (using the 3-dB modal band and 5 low-frequency passbands) are shown in Fig. 15.

Fig. 15 shows three groups of BERs (**a**, **b**, and **c**), as shown in Fig. 12. However, the definitions of Groups **a**, **b**, and **c** in Fig. 15 are not quite the same as those in Fig. 12. In Fig. 12, Groups **a**, **b**, and **c** were defined only visually by how the BER averages seemed to appear in three visually distinct clusters. However, each of those three visually distinct groups represented one of three basic situations: no LBC (Group **a**), LBC with one-bit error correction (Group **b**), and LBC with two-bit error

correction (Group **c**). Importantly, these three situations are used as the new definitions of Groups **a**, **b**, and **c** in Fig. 15. Group **a** (no LBC) results in a data rate of 280 Mbps. When the received optical power ($P_{r,optical,req}$) is higher than -15 dBm, the BER curve is higher than 10^{-7}, so Group **a** is not usable. In Group **b** (one-bit error correction), all five BER curves are lower than 10^{-7} when the received optical power ($P_{r,optical,req}$) is higher than -15 dBm. The maximum data rate of Group **b** is 572 Mbps, which comes from using (31, 26) LBC with Type-I bit allocation. In Group **c** (two-bit error correction), when the received optical power ($P_{r,optical,req}$) is higher than -15 dBm, all four BER curves are lower than 10^{-10}. Therefore, all four cases in Group **c** would be satisfactory in an optical communication system. Group **c**'s maximum data rate of 462 Mbps is obtained when using (31, 26) LBC with Type-I bit allocation. Additionally, at BER = 10^{-10}, Group **c** provides a coding gain of approximately 3 dB compared to Group **b**.

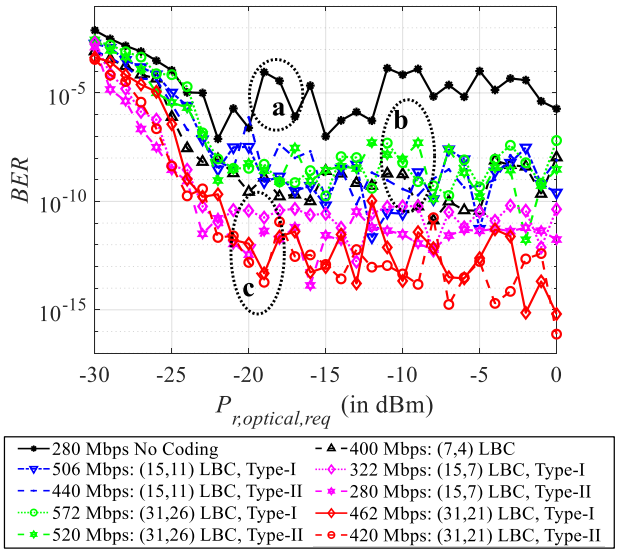

Fig. 15. Average BERs of 10 combinations of LBC and bit allocation when using the 3-dB modal band and 5 low-frequency passbands.

Comparing Fig. 12 and Fig. 15, each of the ten BER curves in Fig. 15 is lower than its corresponding curve in Fig. 12. These results show the effect of how a particular MMF frequency response is utilized because MMF is frequency selective. Specifically, in this communication system, the data rate of each case in Fig. 15 is lower because passband #3 was not used.

C. Simulation of MMF Communication with a 3-dB Modal Band and 4 Low-Frequency Passbands

Because the author of [18] determined that the BERs of passbands #2 to #4 are very high, passband #3 (the highest BER) was removed from the communication system in the previous section, which led to the lower BER curves in Fig. 15. Fig. 13 confirms that eliminating passband #4 would also be good. Therefore, in this next simulation, neither passband #3 nor #4 will be used. The simulation results using only the remaining five low-frequency passbands (#0, #1, #2, #5 and #6) are shown in Fig. 16.

In Fig. 16, the BER curve of Group **a** (without LBC) is still higher than the minimum acceptable BER of 10^{-9} when the received optical power ($P_{r,optical,req}$) is higher than -15 dBm. However, in Group **b**, when the received optical power ($P_{r,optical,req}$) is higher than -15 dBm, all five BER curves are below 10^{-9}, so in this configuration, Group **b** is satisfactory for the optical communication system. The maximum data rate of Group **b** is 494 Mbps, coming from the case of (31, 26) LBC with Type-I bit allocation. In Group **c**, all four BER curves vary in a narrow range, and they are all lower than 10^{-14} when the received optical power ($P_{r,optical,req}$) is higher than -15 dBm, so these BERs can be used in an optical communication system. The maximum data rate in Group **c** comes from the case using (31, 26) LBC with Type-I bit allocation, yielding a data rate of 399 Mbps, double the data rate that can be obtained by using only the 3-dB modal band. Comparing Fig. 12, Fig. 15, and Fig. 16, all combination of LBC and bit allocation can be demonstrated as shown in Table I.

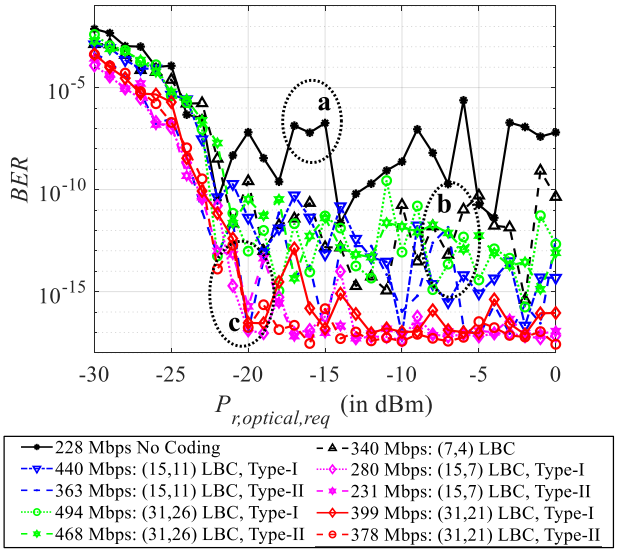

Fig. 16. Average BERs of ten combinations of LBC and bit allocation when using the 3-dB modal band and 4 low-frequency passbands.

From Table I, it is found that the obtained data rate in each combination of LBC and bit allocation when using 3-dB modal band and 4 low-frequency passbands is lower than its corresponding combination of LBC and bit allocation in either when using 3-dB modal band and 5 low-frequency passbands or 3-dB modal band and 6 low-frequency passbands. Moreover, the achieved data rate when using (7, 4) LBC with 3-dB modal band and 5 low-frequency passbands as well as when using (7, 4) LBC with 3-dB modal band and 6 low-frequency passbands are higher than the obtained data rate from [22]. From the table, it is significant to point out that the obtained data rates from applying LBC are higher than those without LBC applied. Additionally, the data rates higher than 600 Mbps can be obtained when applying (31, 26) LBC with 3-dB modal band and 6 low-frequency passbands.

TABLE I: DATA RATE OF ALL COMBINATIONS OF LBC AND BIT ALLOCATION WITH DIFFERENT NUMBERS OF LOW-FREQUENCY PASSBANDS

LBC Types	Data Rate (Mbps)			
	3-dB Modal Band and 6 Low - Frequency Passbands	3-dB Modal Band and 5 Low - Frequency Passbands	3-dB Modal Band and 4 Low - Frequency Passbands	Patmanee et. Al [22]
No Coding	350	280	228	-
(7, 4) LBC	456	400	340	392
(15, 11) LBC, Type-I	583	506	440	-
(15, 11) LBC, Type-II	550	440	363	-
(31, 26) LBC, Type-I	650	572	494	-
(31, 26) LBC, Type-II	624	520	468	-
(15, 7) LBC, Type-I	371	322	280	-
(15, 7) LBC, Type-II	350	280	231	-
(31, 21) LBC, Type-I	525	462	399	-
(31, 21) LBC, Type-II	504	420	378	-

D. The Maximum Data Rate and BER Estimation

To facilitate choosing an optimal MMF communication system, Fig. 17 shows the cubic-fitted data rates and BERs of all three MMF systems discussed above: using the 3-dB modal band and 6 low-frequency passbands, using the 3-dB modal band and 5 low-frequency passbands and using the 3-dB modal band and 4 low-frequency passbands. The cubic fittings in Fig. 17 were obtained using the method described by [26]. Looking first at the MMF system using the 3-dB modal band and 6 low-frequency passbands (the black dashed line), a data rate of 350 to 650 Mbps sent over the MMF will yield BERs between 10^{-9} and 10^{-5}. Looking next at the MMF communication system when using the 3-dB modal band and 5 low-frequency passbands (the blue dotted line), a data rate of 280 to 572 Mbps can provide a BER between 10^{-11} and 10^{-8}. Finally, looking at the MMF communication system when using the 3-dB modal band and 4 low-frequency passbands (the red solid line), a data rate of 231 to 494 Mbps achieves the best BERs of all between 10^{-17} and 10^{-11}.

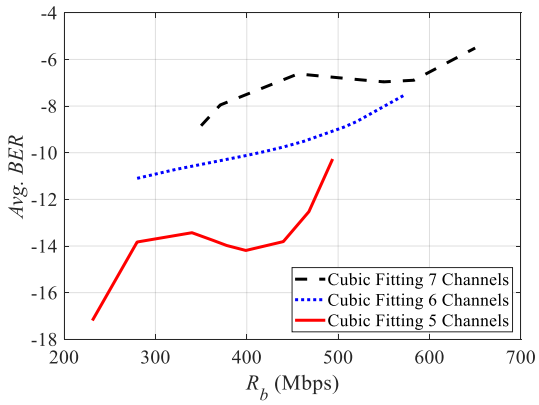

Fig. 17. Cubic-fitted data rates versus BERs of the three transmission settings.

One can see that the estimated BERs decrease while the estimated data rates decrease. The maximum estimated data rate is obtained when using the 3-dB modal band and 6 low-frequency passbands, resulting in the highest BER. On the other hand, the minimum estimated data rate is obtained when using the 3-dB modal band and 4 low-frequency passbands, resulting in the lowest BER (the best one). Fig. 17 can be used to select the suitable communication system with the minimum requirements in terms of the data rate and BER. For example, if the minimum requirements of a particular communication system are a data rate of 400 Mbps and BER value lower than 10^{-10}, the intersection point of data rate = 400 Mbps and BER = 10^{-10} in Fig. 17 must be determined. Once that intersection point is located, then any curve on or below that point can be used for that particular communication system, although of course the lower the better. Therefore, in this example, Fig. 17 shows that the transmission setting with a 3-dB modal band and 6 low-frequency passbands will not be usable because its BER is approximately 10^{-6}, i.e., above the intersection point and too high. On the other hand, using a 3-dB modal band and 5 low-frequency passbands is satisfactory for this requirement (positioned below the intersection point). However, using a 3-dB modal band and 4 low-frequency passbands will have a BER value even lower, approximately 10^{-14}, making it the best choice for this MMF communication system.

V. CONCLUSION

The low-frequency passbands of MMFs have been studied and applied as channels in optical communication. The frequency response of MMFs is frequency selective, resulting in a very high attenuation in signal transmission. This study seeks a way to make low-frequency passbands a viable option for use in MMF communicate on systems. This study develops a method to make effective use of low-frequency passbands by incorporating LBC to greatly reduce corruption from attenuation and thereby obtain attractive BERs. Multiple simulations of the communication system were performed based on a 1-km MMF by applying amplitude shift keying (ASK) and linear block code (LBC). This study uses subcarrier multiplexing (SCM) with a 3-dB modal band and other low-frequency passbands as channels for high data rate transmission. The best results from an MMF communication system using low-frequency passbands were obtained by using the 3-dB modal band and 4 low-frequency passbands. Using (31, 26) LBC and Type-I bit allocation, a data rate of 494 Mbps can

be obtained with a BER lower than 10^{-9}. However, using (31, 21) LBC and Type-I bit allocation, a BER lower than 10^{-14} can be achieved with a data rate of 399 Mbps, which is almost double the data rate that just a 3-dB modal band can send. Significantly, from the optimum configuration studied in this work, a guideline relationship between the obtainable data rates and BERs for different settings is delivered. This relationship can then be used in a variety of MMF communication systems depending on the minimum requirement in terms of the BER and data rate. Additionally, it is seen that the available low-frequency passbands of MMFs are varied from fiber to fiber. It is interesting in the future on how to apply such characteristic to increase the transmission security while keeping the obtained data rates and BERs as required.

CONFLICT OF INTEREST

The authors declare no conflict of interest.

AUTHOR CONTRIBUTIONS

Jaruwat Patmanee developed the system and collected the data as well as wrote the manuscript. Surachet Kanprachar performed the analysis and interpretation of results and wrote the manuscript as well as reviewed the content of the journal. All authors had approved the final version.

FUNDING

This work was supported by Research Fund (Contract No. R2562E003) from Faculty of Engineering, Naresuan University, Phitsanulok, Thailand.

REFERENCES

[1] G. Keiser, *Optical Fiber Communications*, 5th ed. Singapore: McGraw-Hill, 2015, pp. 35-45.

[2] K. Nagashima, *et al*., "A record 1-km MMF NRZ 25.78-Gb/s error-free link using a 1060-nm DIC VCSEL," *IEEE Photonics Technol. Lett.*, vol. 28, no. 4, pp. 418-420, Feb. 2016.

[3] K. Benyahya, *et al*., "Multiterabit transmission over OM2 multimode fiber with wavelength and mode group multiplexing and direct detection," *J. Lightw. Technol.*, vol. 36, no. 2, pp. 355–360, Jan. 2018.

[4] K. Benyahya, *et al*., "High-Speed Bi-Directional transmission over multimode fiber link in IM/DD systems," *J. Lightw. Technol.*, vol. 36, no. 18, pp. 4174–4180, Sept. 2018.

[5] S. Rothe, N. Koukourakis, H. Radner, A. Lonnstrom, E. Jorswieck, and J. W. Czarske, "Physical layer security in multimode fiber optical networks," *Scientific Reports*, vol. 10, no. 1, pp. 1–11, 2020.

[6] S. Rothe, Q. Zhang, N. Koukourakis, and J. Czarske, "Intensity-Only mode decomposition on multimode fibers using a densely connected convolutional network," *Journal of Lightwave Technology*, vol. 39, no. 6, pp. 1672-1679, March 15, 2021.

[7] S. Kanprachar, "Modeling, analysis, and design of subcarrier multiplexing on multimode fiber," Ph.D. dissertation, Dept. Elect. Comp. Eng., Virginia Tech., Blacksburg, VA, USA, 2003.

[8] Y. R. Zheng, *et al*., "DSP implementation of direct sequence spread spectrum underwater acoustic modems with networking capability," in *Proc. Oceans – St. John's*, NL, Canada, Sept. 2014, pp. 1-5.

[9] S. Wang, *et al*., "Compressed receiver for multipath DSSS signals," *IEEE Communication Letters*, vol. 18, no. 8, pp. 1359-1362, Aug. 2014.

[10] A. Pottier, *et al.*, "Quality-of-Service satisfaction games for noncooperative underwater acoustic communications," *IEEE Access*, vol. 6, pp. 21467–21481, 2018.

[11] J. Harshan and Y. Hu., "Cognitive radio from hell: Flipping attack on direct-sequence spread spectrum," in *Proc. IEEE Wireless Communications and Network Conference (WCNC)*, Barcelona, Spain, April 2018, pp. 1-6.

[12] P. I. Puzyrev, *et al*., "Orthogonal multiple chirp modulation for tasks of robust data transmission," in *Proc. 19th International Conference on Young Specialists on Micro/Nanotechnologies and Electron Device (EDM)*, Erlagol, Russia, 2018, pp. 6403-6408.

[13] E. Hugues-Salas, *et al*., "Adaptability-enabled record-high and robust capacity-versus-reach performance of real-time dual-band optical OFDM signals over various OM1/OM2 MMF systems [invited]," *IEEE/OSA J. Opt. Commun. Network.*, vol. 5, no. 10, pp. A1-A11, Oct. 2013.

[14] A. Rahim, *et al.*, "16-channel O-OFDM demultiplexer in silicon photonics," in *Proc. OFC*, San Francisco, CA, USA, 2014, pp. 1-3.

[15] C. T. Tsai, *et al.*, "Multi-Mode VCSEL chip with high-indium-density in GaAs/AlGaAs quantum-well pairs for QAM-OFDM in multi-mode fiber," *IEEE J. Quantum Electron.*, vol. 53, no. 4, Aug. 2017.

[16] Y. Zhu, *et al.*, "Massive grant-free receiver design for OFDM-based transmission over frequency-selective fading channels," in *Proc. 2022 - IEEE International Conference on Communications*, 2022, pp. 2405-2410.

[17] C. Geetha, M. Vanitha, A. Parimala, and D. Kalaiarasi, "A novel channel estimation scheme for MIMO-OFDM systems based on CDD," in *Proc. International Conference on Inventive Computation Technologies*, 2022, pp. 747-753.

[18] J. Patmanee and S. Kanprachar, "Analysis of the multimode fiber at low-frequency passband region," *J. Telecomm. Electron. Comp. Engineering*, vol. 9, no. 2-6, pp. 37–41, 2017.

[19] J. Patmanee, C. Pinthong, and S. Kanprachar, "Performance of subcarrier multiplexing transmission over multimode fiber at low-frequency passbands," in *Proc. IC-ICTES*, Chonburi, Thailand, May 2017, pp. 160-164.

[20] J. Patmanee, C. Pinthong, and S. Kanprachar, "BER performance of multimode fiber low-frequency passbands in subcarrier multiplexing transmission," in *Proc. ICPS*, Chonburi, Thailand, Nov. 2017.

[21] W. E. Ryan and S. Lin, *Channel Codes: Classical and Modern*, New York, USA: Cambridge University Press, 2009, pp. 94-149.
[22] J. Patmanee, C. Pinthong, and S. Kanprachar, "Performance of linear block code with subcarrier multiplexing system on a multimode fiber using low frequency passbands," in *Proc. ECTI-NCON*, Chiang Rai, Thailand, Feb. 2018, pp. 39-44.
[23] S. Kanprachar, *et al*., "High frequency characteristics of multimode fibers with Rayleigh distributed mode delays," *IEANG Trans. Engineering Technol.*, vol. 7, pp. 403-413, 2012.
[24] S. Lin and D. J. Costello, *Error Control Coding*, 2nd ed. Upper Saddle, NU, USA: Pearson Prentice Hall, 2004, pp. 66-95.
[25] J. G. Proakis and M. Salehi, *Digital Communication*, 5th ed. New York, USA: McGraw-Hill, 2008, pp. 400-482.
[26] C. D. Montgomery and C. G. Runger, *Applied Statistics and Probability for Engineers*, John Wiley & Sons, 2014, pp. 494-496.

Jaruwat Patmanee received a B.S., M.S. and Ph.D. degrees in Electrical Engineering from Naresuan University, Phitsanulok, Thailand, in 2014, 2017 and 2022, respectively. He is currently working as lecturer at Faculty of Logistics and Digital Supply Chain, Naresuan University, Phitsanulok, Thailand. His research interests include optical communication systems, coding theory, image processing, and artificial intelligence. His current research is about how to utilize multimode optical fibers in transmitting a very high data-rate signal.

Surachet Kanprachar received his B.Eng. degree (first-class honors) in Electrical Engineering in 1996 from Chulalongkorn University, Bangkok, Thailand. He received M.Sc. and Ph.D. degrees in Electrical Engineering from the Virginia Polytechnic Institute and State University (VA Tech), Blacksburg, Virginia, USA in 1999 and 2003, respectively. Since 2003, he has been with the Department of Electrical and Computer Engineering, Faculty of Engineering, Naresuan University, Phitsanulok, Thailand, where he is now an associate professor. His research interests are in the area of optical fiber communications, coding theory, and artificial intelligence.